UNIVERSITY OF TWENTE.

Faculty of Advanced Technology

Engineering Fluid Dynamics
CTW-TS
Bachelor thesis

The boundary layer of a fluid stream over a flat plate

Date **Januari 2013**

Remco Olimulder

Abstract

In the flow over a solid surface a boundary layer is formed. In this study this boundary layer is investigated theoretically, numerically and experimentally. The equations governing the incompressible laminar flow in thin boundary layers have been derived following Prandtl's theory. For the case of two-dimensional flow over an infinite flat plate at zero incidence, the similarity solution of Blasius is formulated. In addition the similarity solution for the flow stagnating on an infinite flat plate has been derived.

Subsequently the Integral Momentum Equation method of von Kármán is derived. This method is then used to numerically solve for the flow in the boundary layer along the flat plate and for the stagnation-point flow.

For the experimental part of the investigation a wind-tunnel model of a flat plate, of finite thickness, was placed inside the silent wind tunnel. The leading-edge of the wind-tunnel model has a specific smooth shape, designed such that the boundary layer develops like the boundary layer along a plate of infinitesimal thickness. The pressure distribution along the wind-tunnel model, obtained from a CFD calculation has been used as input for the Integral Momentum Equation method to predict the boundary layer development along the model and compare it to Blasius' solution.

The velocity distribution in the boundary layer has been measured using hot-wire anemometry (HWA) at three distances from the leading edge. The data is obtained for three values of the free-stream velocity: 2 m/s, 5m/s and 10m/s, corresponding to different values of the similarity parameter of the boundary layer flow, i.e. the Reynolds number.

The measured velocity profiles are checked on similarity and are compared with the calculated data.

Table of Contents

1. Fluid dynamics

1.1 Boundary layer[1]

"A very satisfactory explanation of the physical process in the boundary layer between a fluid and a solid body could be obtained by the hypothesis of an adhesion of the fluid to the walls, that is, by the hypothesis of a zero relative velocity between fluid and wall." [Ludwig Prandtl, [2]]. So if a fluid flows over a solid body, a boundary layer is formed in which the fluid acts different than in the free stream. Inside this boundary layer, a reduced form of the Navier-Stokes equations can be used to obtain the distribution of the velocity, called the boundary-layer equations. As Ludwig Prandtl stated, inside the boundary layer there is adhesion of the fluid to the walls, thus the flow inside a boundary layer needs to be a viscous flow. The effect of this is that the boundary layer has much influence on the drag of and heat transfer to the body, although the boundary layer is very thin. At the solid surface, the velocity of the fluid and that of the wall must be the same, thus the no-slip condition needs to be imposed. This causes a friction force between adjacent layers of the fluid, trying to equalize their velocities, thus creating a non-linear velocity profile near the fluid-solid boundary.

For a flat plate, x is measured along the length of the plate and y is measured normal to the surface of the plate. The fluid approaches the plate at zero angle of attack with velocity U. This is practically identical to U_∞, the velocity of the fluid above the plate outside the boundary layer. Once the fluid reaches the plate, it will come to a complete stop at the wall, thus building up a boundary layer with a velocity lower than U_∞. Normally the thickness δ of this boundary layer is defined as the distance from the wall where u=0.99 U_∞.

In order to calculate the thickness of the boundary layer some assumptions need to be made. First of all we assume the flow to be 2-dimensional, with coordinates x and y in the 2d plane. We also assume the flow to be incompressible, i.e. $\rho=\rho_\infty$=constant. Furthermore, we assume the flow to be steady, thus no variations in time. Next we assume the fluid to be Newtonian and to have constant properties like viscosity. If we then consider the flow outside the boundary layer to have velocity U_∞, inside the boundary layer the velocity will have 2 components, u is the velocity in x direction and v the velocity in y direction. The Navier-Stokes equations, that give the flow inside the boundary layer, are based on the conservation of mass and momentum. If volumetric forces are neglected, the partial differential equations are:

Mass:
$$\frac{\partial \rho}{\partial t} + \vec{\nabla} \cdot \left(\rho \vec{u} \right) = 0 \tag{1}$$

Momentum:
$$\frac{\partial \rho \vec{u}}{\partial t} + \vec{\nabla} \cdot \left(\rho \vec{u} \vec{u} \right) = \vec{\nabla} \cdot \overline{\overline{\sigma}} \tag{2}$$

With $\overline{\overline{\sigma}} = -p\overline{\overline{I}} + \overline{\overline{\tau}}$ here $\overline{\overline{\tau}}$ is the viscous stress tensor. For a Newtonian fluid

$$\overline{\overline{\tau}} = \mu\left(\vec{\nabla}\vec{u} + \left(\vec{\nabla}\vec{u} \right)^T \right) + \nu\left(\vec{\nabla} \cdot \vec{u} \right)\overline{\overline{I}} \tag{3}$$

with μ and ν viscosity coefficients. According to Stokes' hypothesis the trace of $\overline{\overline{\tau}}$ equals zero, which yields $3\nu+2\mu=0$.

A set of equations can be derived that is specific to the problem. The flow is steady, thus $\frac{\partial}{\partial t}=0$.

Furthermore, it is two dimensional, so

$$\vec{\nabla}=\left(\frac{\partial}{\partial x},\frac{\partial}{\partial y}\right)^T \tag{4}$$

And finally, the flow is incompressible, so ρ is constant. This results in the continuity equation

$$\frac{\partial u}{\partial x}+\frac{\partial v}{\partial y}=0 \tag{5}$$

For the momentum equations, for the case the flow is steady and two dimensional, the *x*-momentum equation becomes

$$\rho\left(u\frac{\partial u}{\partial x}+v\frac{\partial u}{\partial y}\right)=-\frac{\partial p}{\partial x}+\mu\left(\frac{\partial^2 u}{\partial x^2}+\frac{\partial^2 u}{\partial y^2}\right) \tag{6}$$

In the same way the *y*-momentum equation is found to be

$$\rho\left(u\frac{\partial v}{\partial x}+v\frac{\partial v}{\partial y}\right)=-\frac{\partial p}{\partial y}+\mu\left(\frac{\partial^2 v}{\partial x^2}+\frac{\partial^2 v}{\partial y^2}\right) \tag{7}$$

So the governing equations are:

Continuity:
$$\frac{\partial u}{\partial x}+\frac{\partial v}{\partial y}=0 \tag{8}$$

x-momentum:
$$\rho\left(u\frac{\partial u}{\partial x}+v\frac{\partial u}{\partial y}\right)=-\frac{\partial p}{\partial x}+\mu\left(\frac{\partial^2 u}{\partial x^2}+\frac{\partial^2 u}{\partial y^2}\right) \tag{9}$$

y-momentum:
$$\rho\left(u\frac{\partial v}{\partial x}+v\frac{\partial v}{\partial y}\right)=-\frac{\partial p}{\partial y}+\mu\left(\frac{\partial^2 v}{\partial x^2}+\frac{\partial^2 v}{\partial y^2}\right) \tag{10}$$

Before usable results can be found with these equations we will make an essential assumption, that is, that the boundary layer is very thin: $\frac{\delta}{L}\ll 1$. To see the effect of this assumption the three equations are written in non-dimensional form. For this we will use reference parameters *U*,*V*,*L*, δ, *P* and the non-dimensional variables *u**, *v**, *x**, *y**, *p** with

$u=Uu^*,\ v=Vv^*,\ x=Lx^*, y=\delta y^*$ and $p=Pp^*$

The continuity equation then becomes

$$\frac{\partial Uu^*}{\partial Lx^*}+\frac{\partial Vv^*}{\partial \delta y^*}=0\rightarrow\frac{U}{L}\frac{\delta}{V}\frac{\partial u^*}{\partial x^*}+\frac{\partial v^*}{\partial y^*}=0 \tag{11}$$

Because we require the two terms in the equation to be both of order one,

$$\frac{U}{L}\frac{\delta}{V}=1\rightarrow V=U\frac{\delta}{L}\ll U \tag{12}$$

The same can be done with the *x*-momentum equation giving

$$\rho\frac{U^2}{L}\left(u^*\frac{\partial u^*}{\partial x^*}+v^*\frac{\partial u^*}{\partial y^*}\right)=\frac{-P}{L}\frac{\partial p^*}{\partial x^*}+\mu U\left(\frac{1}{L^2}\frac{\partial^2 u^*}{\partial x^{*2}}+\frac{1}{\delta^2}\frac{\partial^2 u^*}{\partial y^{*2}}\right) \tag{13}$$

Re-arranging gives

$$u^*\frac{\partial u^*}{\partial x^*}+v^*\frac{\partial u^*}{\partial y^*}=\frac{-P}{\rho U^2}\frac{\partial p^*}{\partial x^*}+\frac{\mu L}{\rho U\delta^2}\left(\frac{\delta^2}{L^2}\frac{\partial^2 u^*}{\partial x^{*2}}+\frac{\partial^2 u^*}{\partial y^{*2}}\right) \tag{14}$$

The assumption made leads to $\frac{\delta^2}{L^2}\ll 1$, thus the equation becomes

$$u^*\frac{\partial u^*}{\partial x^*}+v^*\frac{\partial u^*}{\partial y^*}=\frac{-P}{\rho U^2}\frac{\partial p^*}{\partial x^*}+\frac{\mu L}{\rho U\delta^2}\frac{\partial^2 u^*}{\partial y^{*2}} \tag{15}$$

Again we need both sides to be of order one. So we need $\frac{P}{\rho U^2}=1$ and $\frac{\mu L^2}{\rho UL\delta^2}=\frac{L^2}{\delta^2}\frac{1}{\mathrm{Re}_L}=1$, thus giving, with $\mathrm{Re}_L=\frac{\rho UL}{\mu}$:

$$P=\rho U^2 \tag{16}$$

$$\frac{\delta^2}{L^2}=\mathrm{Re}_L \tag{17}$$

The above equation states that the scaling of the thickness of the boundary layer is

$$\frac{\delta}{L}=O\left(\mathrm{Re}_L^{\frac{1}{2}}\right) \tag{18}$$

Transforming everything back to the dimensionful form, the *x*-momentum equation now reads:

$$\rho\left(u\frac{\partial u}{\partial x}+v\frac{\partial u}{\partial y}\right)=-\frac{\partial p}{\partial x}+\mu\frac{\partial^2 u}{\partial y^2} \tag{19}$$

A comparable analysis can be applied to the y-momentum equation. It then reads:

$$0=-\frac{\partial p}{\partial y}\rightarrow p=p(x) \tag{20}$$

So the pressure is apparently constant in the boundary layer along lines for which *x*=constant, i.e.

p(x) is the pressure specified at the edge of the boundary layer. The final equations for *u(x,y)* and *v(x,y)* inside the boundary layer then become:

$$\frac{\partial u}{\partial x}+\frac{\partial v}{\partial y}=0 \tag{21}$$

$$\rho\left(u\frac{\partial u}{\partial x}+v\frac{\partial u}{\partial y}\right)=-\frac{dp}{dx}+\mu\frac{\partial^2 u}{\partial y^2} \tag{22}$$

1.2 Boundary conditions

We also need boundary conditions to be able to solve these partial differential equations. If we consider the boundary layer, we note that for every *x*, *u* needs to be 0 for *y*=0 because of the no-slip boundary condition. The same is true for *v*. The third boundary condition can be found at the edge of the boundary layer. Because we defined δ to be the thickness of the boundary layer, $u \rightarrow U_\infty$ for every *x* when $y \geq \delta$. So the boundary conditions are: $u(x,0)=0$, $u(x,\infty)=U$, $v(x,0)=0$.

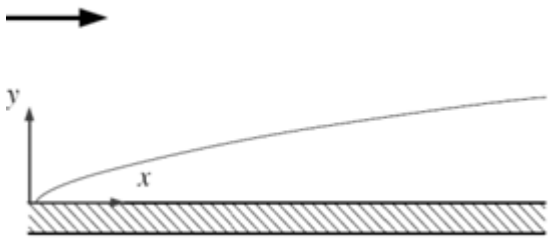

Figure 1.1 The boundary layer according to Blasius[1]

Furthermore, at the edge of the boundary layer: $\frac{\partial u}{\partial y}=0$, $\frac{\partial^2 u}{\partial y^2}=0$, etcetera.

Note that it follows from Eq.(22) that at the edge of the boundary layer, where $u(x,y\rightarrow\infty)=U(x)$, for the given boundary conditions

$$\frac{dp}{dx}=-\rho U\frac{dU}{dx} \tag{23}$$

1.3 Blasius' Solution[3]

In order to obtain an exact solution, we introduce a stream function Ψ(x,y), with

$$u(x,y)=\frac{\partial \psi}{\partial y};v(x,y)=-\frac{\partial \psi}{\partial x} \tag{24}$$

This satisfies the continuity equation, Eq. (21) exactly. In the case of the flat plate boundary layer, $U(x)\equiv \text{constant}$, so that it follows from Eq.(23) that $\frac{dp}{dx}=0$. If eq. (24) then is substituted in to the *x*-momentum equation, we find:

$$\frac{\partial \psi}{\partial y}\frac{\partial^2 \psi}{\partial x\partial y}-\frac{\partial \psi}{\partial x}\frac{\partial^2 \psi}{\partial y^2}=\frac{\mu}{\rho}\frac{\partial^3 \psi}{\partial y^3} \tag{25}$$

Since there is no length scale in the problem, it is to be expected that a similarity solution is a possibility for this equation. A similarity solution for this equation can be found if *Ψ(x,y)* is expressed as

$$\psi(x,y) = Ax^p f(\eta) \tag{26}$$

$$\text{With } \eta(x,y) = Byx^q \tag{27}$$

Which should lead to an ordinary differential equation for *f(η)*not containing coefficients that depend on *x*. Substituting the expression for *Ψ(x,y)* , the momentum equation then gives the following equation

$$(p+q) f'^2 - pff'' = \frac{\mu}{\rho}\frac{B}{A} x^{-p+q+1} f''' \tag{28}$$

This needs to be a similarity solution, a solution independant of *x*. So we need

$$-p+q+1=0 \tag{29}$$

For convenience we choose

$$\frac{\mu}{\rho}\frac{B}{A} = 1 \rightarrow A = B\frac{\mu}{\rho} \tag{30}$$

Also the boundary conditions need to be satisfied. For this we use

$$u(x,y) = \frac{\partial \psi}{\partial y} = ABx^{p+q} f' \tag{31}$$

$$\begin{aligned} v(x,y) &= -\frac{\partial \psi}{\partial x} = -\left(Apx^{p-1} f + ABqyx^{p+q-1} f'\right) \\ &= -Ax^{p-1}\left(pf + q\eta f'\right) \end{aligned} \tag{32}$$

For $u(x,0) = 0 \rightarrow f'(0) = 0$, $v(x,0) = 0 \rightarrow f(0) = 0$.The final boundary condition is satisfied when

$$u(x,\infty) = U_\infty \rightarrow \frac{\partial \psi}{\partial y} = ABx^{p+q} f'(\infty) = U \tag{33}$$

This will be a similarity solution only if $x^{p+q} = 1 \rightarrow p+q = 0$

Using the two equations for *p* and *q* it can be found that $p = \frac{1}{2}; q = -\frac{1}{2}$

Also, $AB = U$ and $f'(\infty) = 1$ Using Eq.(30), i.e. $A = B\frac{\mu}{\rho}$ it follows $B = \sqrt{\frac{\rho U}{\mu}}$ and $A = \sqrt{\frac{\mu U}{\rho}}$

Thus Blasius' equation is the solution of

$$2\frac{d^3 f}{d\eta^3} + f\frac{d^2 f}{d\eta^2} = 0 \tag{34}$$

This is a third-order, nonlinear ordinary differential equation and three boundary conditions are needed to solve this. These conditions were derived above:

$$f(0) = 0$$

$$f'(0) = 0$$

$$f'(\infty) = 1$$

The third-order ordinary differential equation can be expressed as an initial value problem involving a system of three first order ordinary differential equations for *f*, *f'* and *f"*.

$$\frac{df}{d\eta} = f' \qquad \text{With } f(0) = 0 \qquad (35)$$

$$\frac{df'}{d\eta} = f'' \qquad \text{With } f'(0) = 0 \qquad (36)$$

$$\frac{df''}{d\eta} = -\tfrac{1}{2} ff'' \qquad \text{with } f''(0) = ? \qquad (37)$$

This indicates that a third initial condition is needed, namely $f''(0)$. Because instead we know $f'(\infty) = 1$ the "shooting technique" is used. In this technique a $f''(0)$ is varied in order to find a solution that satisfies $f'(\infty) = 1$. It is found that the initial condition $f''(0) = 0.332$ satisfies this condition.

The solution for $u(x, y)/U = f'(\eta)$ is shown in figure 1.2 below. It shows a similarity solution which tends to $f' = 1$ for $\eta \to \infty$

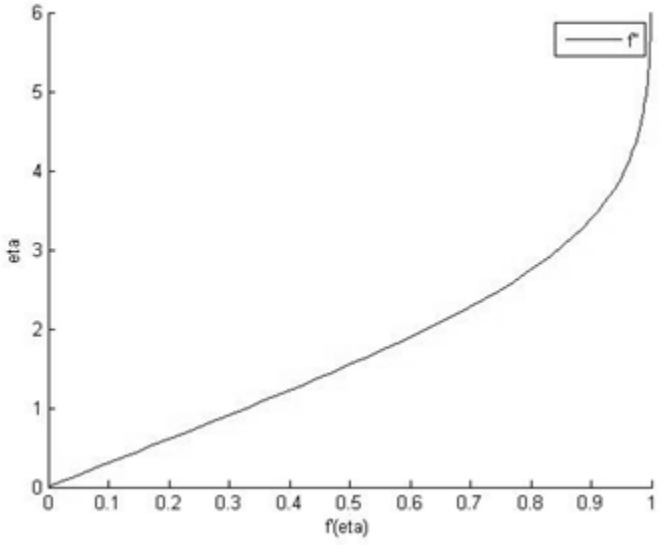

Figure 1.2 Blasisus' solution of velocity profile in boundary layer over flat plate at zero incidence

From the numerical solution it is determined that u=0.99U is reached when η =4.91,

furthermore: $f(\eta \to \infty) \to \eta - 1.63188$

The stream function becomes

$$\psi(x,y) = Ux(\mu/\rho Ux)^{1/2} f(\eta) = \frac{Ux}{\mathrm{Re}_x^{1/2}} f(\eta) \tag{38}$$

$$\text{with } \eta(x,y) = \frac{y}{x}\left(\frac{\rho Ux}{\mu}\right)^{1/2} = \frac{y}{x}\mathrm{Re}_x^{1/2} \tag{39}$$

If we then want to find the boundary layer thickness we use that $\eta \approx 4.91$ and $y = \delta_{u=0.99U}$ to find

$$\delta(x) = 4.91x\Big/\left(\frac{\rho Ux}{\mu}\right)^{1/2} = \frac{4.91x}{\mathrm{Re}_x^{1/2}} \tag{40}$$

Also, two other parameters which are commonly used to measure the properties of a boundary layer are the displacement thickness δ^*, Eq.(41) and the momentum thickness ϑ, Eq.(42)

$$\delta^*(x) = \int_0^\delta \left(1 - \frac{u}{U}\right) dy \tag{41}$$

$$\theta(x) = \int_0^\infty \frac{u}{U}\left(1 - \frac{u}{U}\right) dy \tag{42}$$

For flat plate boundary layer flow, the displacement thickness $\delta^*(x)$, can be calculated to give

$\delta^*(x) = \frac{x}{\mathrm{Re}_x^{1/2}} \int_0^\delta \left(1 - f'(\eta)\right) d\eta$, and the momentum thickness, $\vartheta(x)$, can be calculated to give

$$\theta(x) = \frac{x}{\mathrm{Re}_x^{1/2}} \int_0^\infty f'(\eta)\left(1 - f'(\eta)\right) d\eta$$

Summarizing the similarity solution of Blasius:

$$\psi(x,y) = \frac{Ux}{\mathrm{Re}_x^{1/2}} f(\eta)$$

$$u(x,y) = Uf'(\eta)$$

$$v(x,y) = \frac{-U}{2\,\mathrm{Re}_x^{1/2}}\left(f(\eta) - \eta f'(\eta)\right) \to v(x, y \to \infty) = \frac{U}{\mathrm{Re}_x^{1/2}} 0.8659$$

$$\tau_w(x) = \mu\left(\frac{\partial u}{\partial y}\right)_0 = \frac{\rho U^2}{\mathrm{Re}_x^{1/2}} f''(0) \to \frac{\frac{1}{2}\rho U^2}{\mathrm{Re}_x^{1/2}} 0.664 \to C_f(x) = \frac{0.664}{\mathrm{Re}_x^{1/2}}$$

$$\delta^*(x) = \frac{x}{\mathrm{Re}_x^{1/2}} \int_0^\delta \left(1 - f'(\eta)\right) d\eta = \frac{x}{\mathrm{Re}_x^{1/2}} 1.7269$$

$$\theta(x) = \frac{x}{\mathrm{Re}_x^{1/2}} \int_0^\infty f'(\eta)\left(1 - f'(\eta)\right) d\eta = \frac{x}{\mathrm{Re}_x^{1/2}} 0.6656$$

1.4 Stagnation point flow

The method that Blasius used can also be used to find a similarity solution for the stagnation point flow. The same stream function as used for Blasius' solution (Eq. (24)) can be used. If Eq. (24) is substituted in the x-momentum equation, using that $-\frac{1}{\rho}\frac{dp}{dx}=U\frac{dU}{dx}$ it gives:

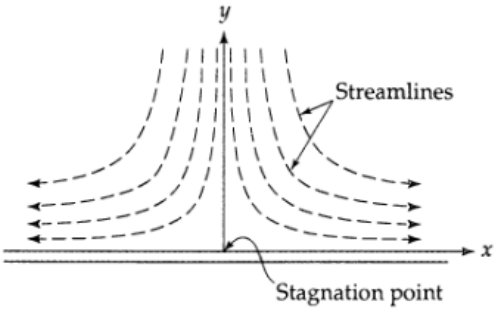

Figure 1.3 Stagnation point type of flow[4]

$$\frac{\partial\psi}{\partial y}\frac{\partial^2\psi}{\partial x\partial y}-\frac{\partial\psi}{\partial x}\frac{\partial^2\psi}{\partial y^2}=\frac{\mu}{\rho}\frac{\partial^3\psi}{\partial y^3}+U\frac{dU}{dx} \tag{43}$$

Since there is no length scale in the problem, again a similarity solution is expected to be a possibility. A similarity solution for this equation can be found if *Ψ(x,y)* is expressed as

$$\psi(x,y)=Ax^p f(\eta) \tag{44}$$

$$\text{With } \eta(x,y)=Byx^q \tag{45}$$

Substituting the expression for *Ψ(x,y)* in the momentum equation, and using that $U=cx$ so that $\frac{dU}{dx}=c$ this then gives the following equation:

$$(p+q)f'^2-pff''=\frac{\mu}{\rho}\frac{B}{A}x^{-p+q+1}f'''+\left(\frac{c^2}{A^2B^2}\right)x^{-2p-2q+2} \tag{46}$$

The solution of this ODE needs to be a similarity solution, a solution independent of x. So we need

$$-p+q+1=0 \tag{47}$$

$$-2p-2q+2=0 \tag{48}$$

Using the two equations for *p* and *q* it can be found that $p=1;q=0$ resulting in

$\psi(x,y)=Axf(\eta)$

With $\eta(x,y)=By$

For convenience we choose

$$\frac{\mu}{\rho}\frac{B}{A}=1\rightarrow A=B\frac{\mu}{\rho} \tag{49}$$

thus the similarity solution for the stagnation point flow will be a solution of the differential equation

$$f'^2-ff''=f'''+\frac{c^2}{A^2B^2} \tag{50}$$

Also the boundary conditions need to be satisfied. For this we use

$$u(x,y)=\frac{\partial\psi}{\partial y}=ABxf' \tag{51}$$

$$v(x,y)=-\frac{\partial\psi}{\partial x}=-Af \tag{52}$$

For $u(x,0)=0\rightarrow f'(0)=0$, $v(x,0)=0\rightarrow f(0)=0$.The final boundary condition is satisfied when

$$u(x,\infty)=cx\rightarrow ABxf'(\infty)=cx \tag{53}$$

So that choosing $AB=c$ will satisfy the ODE only if $f'(\infty)=1$.

using $A=B\frac{\mu}{\rho}$ it follows $B=\sqrt{\frac{\rho c}{\mu}}$ and $A=\sqrt{\frac{\mu c}{\rho}}$

Thus the stagnation point similarity solution is the solution of

$$f'^2-ff''-f'''=1 \tag{54}$$

This is a third order, nonlinear ordinary differential equation and three boundary conditions are needed to solve this. These conditions were derived above:

$$f(0)=0$$

$$f'(0)=0$$

$$f'(\infty)=1$$

The third order ordinary differential equation can be expressed as an initial value problem involving a system of three first order ordinary differential equations for *f, f'* and *f"*.

$$\frac{df}{d\eta}=f' \qquad \text{With } f(0)=0 \tag{55}$$

$$\frac{df'}{d\eta}=f'' \qquad \text{With } f'(0)=0 \tag{56}$$

$$\frac{df''}{d\eta}=f'^2-ff''-1 \qquad \text{with } f''(0)=? \tag{57}$$

Again the "shooting technique" is used. It is found that the initial condition $f''(0)=1.233$ satisfies this condition.

The solution for $u(x,y)/cx=f'(\eta)$ is presented in figure 1.4 below. It shows a similarity solution which tends to $f'=1$ for $\eta\rightarrow\infty$

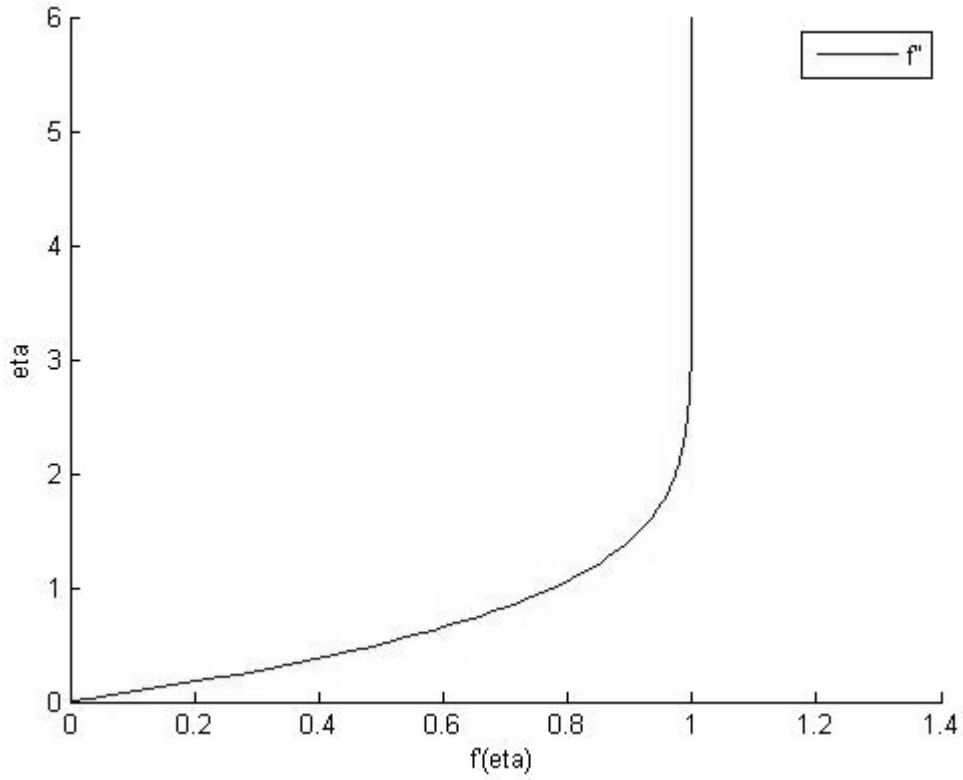

Figure 1.4Blasisus' solution of velocity profile in boundary layer stagnation point flow

From the numerical solution it is determined that *u*=0.99*cx* is reached when η =2.36. Furthermore $f(\eta \to \infty) \to \eta - 0.64967$

The stream function becomes

$$\psi(x,y) = \sqrt{\frac{\mu c}{\rho}} x f(\eta) \tag{58}$$

$$u(x,y) = cxf'(\eta) \tag{59}$$

$$v(x,y) = -\sqrt{\frac{\mu c}{\rho}} f(\eta) \to v(x, y \to \infty) = -cy \tag{60}$$

$$\text{with } \eta(x,y) = \sqrt{\frac{\rho c}{\mu}} y \tag{61}$$

Then also the skin friction, $\tau_w(x) = \mu \left(\frac{\partial u}{\partial y} \right)_{y=0}$, can be found. Because $\left(\frac{\partial u}{\partial y} \right)_{y=0} = AB^2 x f''(0)$ this thus gives $\tau_w(x) = \mu c \sqrt{\frac{c\rho}{\mu}} x f''(0) = \rho c \sqrt{\frac{\mu c}{\rho}} x f''(0)$

If we then want to find the boundary layer thickness we use that $\eta \approx 2.36$ and $y = \delta_{u=0.99U}$ to find

$$\delta(x) = 2.36 \sqrt{\frac{\mu}{\rho c}} \tag{62}$$

This solution is a constant. So the boundary layer thickness in a stagnation type of flow turns out to be constant.

Summarizing the similarity solution of the stagnation point flow:

$$\psi(x,y) = \sqrt{\frac{\mu c}{\rho}} x f(\eta)$$

$$u(x,y) = cxf'(\eta) \rightarrow u(x, y \rightarrow \infty) = cx$$

$$v(x,y) = -\sqrt{\frac{\mu c}{\rho}} f(\eta) \rightarrow v(x, y \rightarrow \infty) = -cy + \sqrt{\frac{\nu}{c}} 0.64967$$

$$\tau_w(x) = \mu \left(\frac{\partial u}{\partial y} \right)_0 = \tfrac{1}{2} \rho c x \sqrt{\frac{\mu c}{\rho}} 2 f''(0) \rightarrow C_f = \frac{cx\sqrt{\nu c}}{U_{ref}^2} 2.466$$

$$\delta^*(x) = \sqrt{\frac{\nu}{c}} \int_0^{\delta} \left(1 - f'(\eta)\right) d\eta = \sqrt{\frac{\nu}{c}} 0.64717$$

$$\theta(x) = \sqrt{\frac{\nu}{c}} \int_0^{\infty} f'(\eta) \left(1 - f'(\eta)\right) d\eta = \sqrt{\frac{\nu}{c}} 0.29196$$

2. Numerical technique in solving boundary layer equations

2.1 Von Kármán momentum integral method[5]

Exact solutions to the boundary layer equations can only be found in simple cases, such as the steady flow over a flat plate at zero angle of attack. For that situation we found Blasius' solution. For more complicated cases a numerical method can be used to give an approximation of the solution of the flow in the boundary layer. A much used technique is the Von Kármán integral momentum equation. This equation considers the boundary layer equations integrated over the thickness of the boundary layer. From the x-momentum equation (Eq. (23)) applied at the edge of the boundary layer it followed that $U\frac{dU}{dx}=-\frac{1}{\rho}\frac{dp}{dx}$ .The Von Kármán integral momentum equation can be found by integrating the momentum equation,

$$u\frac{\partial u}{\partial x}+v\frac{\partial u}{\partial y}=U\frac{dU}{dx}+\nu\frac{\partial^2 u}{\partial y^2} \tag{63}$$

Adding and subtracting $u\,dU/dx$, we get

$$(U-u)\frac{dU}{dx}+u\frac{\partial(U-u)}{\partial x}+v\frac{\partial(U-u)}{\partial y}=-\nu\frac{\partial^2 u}{\partial y^2} \tag{64}$$

If we integrate then from y=0 to y=h, with $h>\delta$, the right hand side of this equation becomes

$$-\nu\int_0^h\frac{\partial^2 u}{\partial y^2}dy=\nu\left(\frac{\partial u}{\partial y}\right)_0=\frac{\tau_w}{\rho} \tag{65}$$

Here τ_0 is the wall shear stress. The first part of the left hand side becomes

$$\int_0^h(U-u)\frac{dU}{dx}dy=\frac{dU}{dx}\int_0^h(U-u)dy=\frac{dU}{dx}U\delta^* \tag{66}$$

With $\delta^*(x)$, the boundary layer displacement thickness, defined in Eq.(41).
The third part of the left hand side, upon partial integration and using the continuity equation, becomes

$$\int_0^h v\frac{\partial(U-u)}{\partial y}dy=v(U-u)\Big|_0^h-\int_0^h(U-u)\frac{\partial v}{\partial y}dy \tag{67}$$

$$=0+\int_0^h(U-u)\frac{\partial u}{\partial x}dy \tag{68}$$

The integral momentum equation is then

$$\frac{dU}{dx}U\delta^*+\int_0^h\left[u\frac{\partial(U-u)}{\partial x}+\frac{\partial u}{\partial x}(U-u)\right]dy=\frac{\tau_w}{\rho} \tag{69}$$

the second part of this equation can be rewritten

$$\int_0^h \left[u\frac{\partial(U-u)}{\partial x} + \frac{\partial u}{\partial x}(U-u) \right] dy = \int_0^h \left[\frac{\partial}{\partial x} u(U-u) \right] dy \tag{70}$$

$$\int_0^h \left[\frac{\partial}{\partial x} u(U-u) \right] dy = \frac{d}{dx}\int_0^h \left[u(U-u) \right] dy = \frac{d}{dx}\left(U^2\theta\right) \tag{71}$$

With ϑ the boundary layer momentum thickness, defined in Eq.(42). Substituting this in the integrated momentum equation yields:

$$\frac{dU}{dx}U\delta^* + \frac{d}{dx}\left(U^2\theta\right) = \frac{\tau_w}{\rho} \tag{72}$$

This is called the von Kármán integral momentum equation which is valid for both laminar and turbulent boundary layers. However, it is easiest for laminar boundary layers because in that case the wall shear stress is equal to the molecular viscosity times the velocity gradient at the wall.

2.2 Velocity profile

The von Kármán integral momentum equation can be used employing some choosen velocity profile, satisfying as many boundary conditions as possible. In the present study we assume a cubic velocity profile

$$\frac{u(x,y)}{U} = a + b\frac{y}{\delta} + c\frac{y^2}{\delta^2} + d\frac{y^3}{\delta^3} \tag{73}$$

With $\delta=\delta(x)$, the yet unknown boundary layer thickness at x, and a,b,c and d constants.
This profile has four unknown constants, so four boundary conditions are needed. At y=0 we have $u(x,0)$=0 because of the no-slip boundary condition and from the x-momentum equation we derive

$$\left(\partial^2 u/\partial y^2\right)_{y=0} = \frac{1}{\mu}\frac{dp}{dx} \tag{74}$$

The other two conditions can be found in the free stream. If $y \geq \delta$ we have $u=U$ and because in y-direction u is the same everywhere along the line x=constant in the free stream $\left(\partial u/\partial y\right) = 0$.
imposing these boundary conditions gives the following constants

$$0 = a \qquad b = \frac{3}{2} - \frac{1}{4}\frac{\delta^2}{\mu U}\frac{dP}{dx} \qquad c = \frac{\delta^2}{2\mu U}\frac{dP}{dx} \qquad d = -\frac{1}{2} - \frac{1}{4}\frac{\delta^2}{\mu U}\frac{dP}{dx}$$

When these are substituted in the velocity profile, after some rewriting, it follows

$$\frac{u(x,y)}{U(x)} = \frac{3}{2}\frac{y}{\delta} - \frac{1}{2}\frac{y^3}{\delta^3} + \frac{1}{4}\frac{\delta^2}{\mu U}\frac{dP}{dx}\left(-\frac{y}{\delta} + 2\frac{y^2}{\delta^2} - \frac{y^3}{\delta^3}\right) \tag{75}$$

substituting $\frac{dP}{dx} = -\rho U \frac{dU}{dx}$ gives $\frac{u(x,y)}{U(x)} = \frac{3}{2}\frac{y}{\delta} - \frac{1}{2}\frac{y^3}{\delta^3} + \frac{1}{4}\frac{\delta^2\rho}{\mu}\frac{dU}{dx}\left(\frac{y}{\delta} - 2\frac{y^2}{\delta^2} + \frac{y^3}{\delta^3}\right)$

With $\delta=\delta(x)$, the quantity that is to be determined from the von Kármán integral momentum equation. Substituting the velocity profile in the definitions of δ^*, ϑ and τ_w gives

$$\delta^* = \delta\left[\frac{3}{8} - \frac{1}{48}\frac{\rho\delta^2}{\mu}\frac{dU}{dx}\right]$$

$$\theta = \delta\left[\frac{39}{280} - \frac{1}{140}\left(\frac{\delta^2}{4\nu}\frac{dU}{dx}\right) - \frac{1}{105}\left(\frac{\delta^2}{4\nu}\frac{dU}{dx}\right)^2\right]$$

$$\tau_w = \frac{\mu U}{\delta}\left(\frac{3}{2} + \frac{\delta^2}{4\nu}\frac{dU}{dx}\right)$$

Then substituting in the von Kármán integral momentum equation and rewriting gives

$$\left[\begin{array}{l} \nu\frac{39}{280}U\frac{d\delta}{dx} - \frac{3}{560}\delta^2 U\frac{dU}{dx}\frac{d\delta}{dx} - \\ \frac{5}{1680}\frac{1}{\nu}\delta^4 U\left(\frac{dU}{dx}\right)^2\frac{d\delta}{dx} \end{array}\right] = \left[\begin{array}{l} \nu^2\frac{3}{2}\frac{1}{\delta} - \nu\frac{113}{280}\delta\frac{dU}{dx} + \frac{1}{560}\delta^3 U\frac{d^2U}{dx^2} + \\ \frac{41}{1680}\delta^3\left(\frac{dU}{dx}\right)^2 + \frac{2}{1680}\frac{1}{\nu}\delta^5\left(\frac{dU}{dx}\right)^3 + \frac{2}{1680}\frac{1}{\nu}\delta^5 U\frac{dU}{dx}\frac{d^2U}{dx^2} \end{array}\right] \quad (76)$$

Then both sides are multiplied with δ and $\frac{d\delta^2}{dx}$ is taken out of the brackets. The equation then reads

$$f_1(\delta)\frac{d\delta^2}{dx} = f_2(\delta) \rightarrow \frac{d\delta^2}{dx} = \frac{f_2(\delta)}{f_1(\delta)} \quad (77)$$

$$f_1(\delta) = \left(\frac{39}{560} - \frac{3}{1120}\frac{1}{\nu}\delta^2\frac{dU}{dx} - \frac{1}{672}\frac{1}{\nu^2}\delta^4\left(\frac{dU}{dx}\right)\right)^2 \nu U \quad (78)$$

$$f_2(\delta) = \left[\begin{array}{l} \nu^2\frac{3}{2} - \nu\frac{113}{280}\frac{dU}{dx}\delta^2 + \left(\frac{1}{560}U\frac{d^2U}{dx^2} + \frac{41}{1680}\left(\frac{dU}{dx}\right)^2\right)\delta^4 + \\ \left(\frac{2}{1680}\frac{1}{\nu}\left(\frac{dU}{dx}\right)^3 + \frac{2}{1680}\frac{1}{\nu}U\frac{dU}{dx}\frac{d^2U}{dx^2}\right)\delta^6 \end{array}\right] \quad (79)$$

This equation can then be solved numerically for δ^2 using a simple Euler scheme

$$\frac{d\delta^2}{dx} = \frac{\delta_{i+1}^2 - \delta_i^2}{\Delta x} = \frac{f_2\left(\delta_i^2\right)}{f_1\left(\delta_i^2\right)} \rightarrow \delta_{i+1}^2 = \frac{f_2\left(\delta_i^2\right)}{f_1\left(\delta_i^2\right)}\Delta x + \delta_i^2 + O\left(\Delta x^2\right) \quad (80)$$

For i=0,1,.... and given δ_0^2

For the flat plate without pressure gradient, this leads to

$$f_1\left(\delta^2\right)=\nu\frac{39}{560}U;\ f_2\left(\delta^2\right)=\nu^2\frac{3}{2} \tag{81}$$

$$\frac{d\delta^2}{dx}=\frac{\nu^2\frac{3}{2}}{\nu\frac{39}{560}U}=\frac{\nu}{U}\frac{3}{2}\frac{560}{39}=\frac{\nu}{U}\frac{280}{13} \tag{82}$$

With the boundary condition $\delta^2=0$ for x=0.
In this case the von Kármán integral momentum equations can be solved analytically

$$\delta^2(x)=\frac{\nu}{U}\frac{280}{13}x\rightarrow\delta(x)=\sqrt{\frac{\nu}{Ux}}\sqrt{\frac{280}{13}}x=\sqrt{\frac{280}{13}}\frac{x}{\mathrm{Re}_x^{1/2}}=4.64\frac{x}{\mathrm{Re}_x^{1/2}} \tag{83}$$

This is in good agreement with Blasius' result of $\delta(x)=4.91\frac{x}{\mathrm{Re}_x^{1/2}}$

Furthermore, δ^*, ϑ and C_f can be compared for von Kármán and Blasius giving

Von Kármán	Blasius
$\delta(x)=4.64\frac{x}{\mathrm{Re}_x^{1/2}}$	$\delta(x)=4.91\frac{x}{\mathrm{Re}_x^{1/2}}$
$\delta^*=1.74\frac{x}{\mathrm{Re}_x^{1/2}}$	$\delta^*=1.73\frac{x}{\mathrm{Re}_x^{1/2}}$
$\theta=0.643\frac{x}{\mathrm{Re}_x^{1/2}}$	$\theta=0.666\frac{x}{\mathrm{Re}_x^{1/2}}$
$c_f(x)=0.646\frac{1}{\mathrm{Re}_x^{1/2}}$	$c_f(x)=0.664\frac{1}{\mathrm{Re}_x^{1/2}}$

These also show a good agreement of the result predicted by von Karman and Blasius.

3. Numerical results of von Kármán integral momentum equation

3.1 Flat plate

For a flat plate of infinitesimal thickness inserted into a fluid stream at zero incidence we now have two theoretical solutions. The first one is Blasius' solution

$$\delta = 4.91x \Big/ \left(\frac{\rho U x}{\mu} \right)^{1/2} \tag{84}$$

The second one is the analytical solution of the von Kármán integral momentum equation $\delta(x) = 4.64 \frac{x}{\mathrm{Re}_x^{1/2}}$. The numerical solution follows from $\delta_{i+1}^2 = \delta_i^2 + \Delta x \frac{280}{13} \frac{\nu}{U}$

$$\delta_{i+1} = \sqrt{\frac{280}{13} \frac{\mu}{\rho U} \Delta x + \delta_i^2} \text{ for i=0,1,2,…..} \tag{85}$$

3.1.1 Stepsize

If the numerical solution is analyzed, it can be seen that it depends on a step size Δx. This implies that taking a different value for Δx will change the accuracy of δ_{i+1} and thus the accuracy of the numerical solution. In this case $\frac{d\delta^2}{dx}$ is evaluated which implies that the Euler scheme yields the exact solution of the von Kármán integral momentum equation. Thus the accuracy is independent of Δx.

3.1.2 Comparison of the numerical solution with Blasius' solution

Using the numerical method the boundary layer thickness is obtained. In figure 3.1 this solution is compared with Blasius' solution.

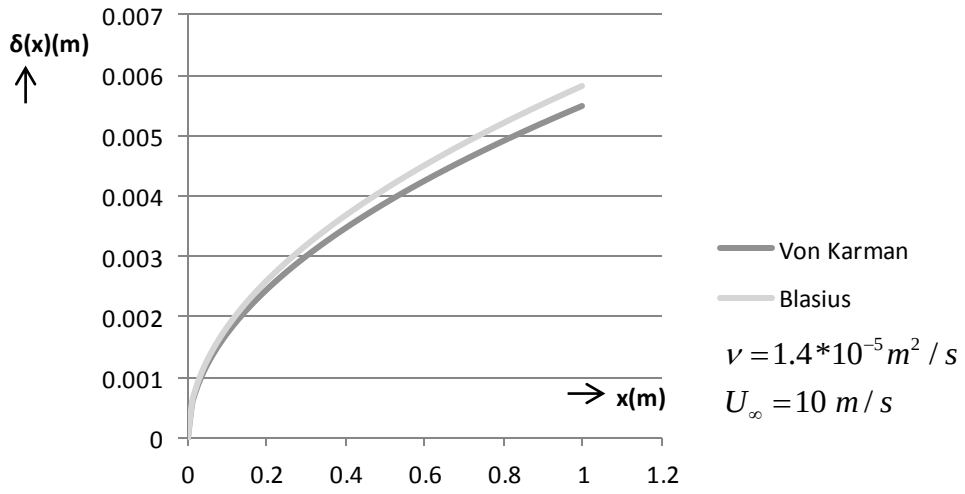

Figure 3.1 Comparison of Blasius' solution with the numerical solution for Δx=0.01

As we can see in the figure, the two solutions have a similar shape. However, the numerical solution does give a smaller thickness of the boundary layer. The difference between Blasius' solution and the solution of the von Kármán integral momentum equation is a constant percentage of Blasius' solution. The difference in thickness according to the von Kármán integral momentum equation and Blasius' solution can be calculated and is $\frac{\sqrt{\frac{280}{13}}-4.91}{4.91}\cdot 100\% = 5.47\%$. Thus the boundary layer thickness according to the von Kármán integral momentum equation is 5.5% smaller than the thickness found with Blasius' equation.

3.2 Stagnation point flow

As seen in the preceding chapter, the numerical solution is a good approximation to the analytical solution. Because of this the numerical solution can be used to approximate solutions for cases for which an analytical solution of the von Karman momentum integral equation cannot be found. This is the case for another important flow, namely the stagnation point flow. Stagnation point flow occurs when an object with a finite thickness is placed in a fluid stream. The easiest case is when a flat surface is placed in a fluid stream, with the surface perpendicular to the free stream velocity. In that case the boundary conditions for the von Kármán integral momentum equation are the same for the flat plate at zero incidence. However, because now $U = cx; \frac{dU}{dx} = c$, this time $\frac{dU}{dx}$ is not equal to zero and has to be taken into account. The von Kármán integral momentum equation for $\frac{d\delta^2}{dx} = \frac{f_2\left(\delta^2\right)}{f_1\left(\delta^2\right)}$ is thus

$$f_1\left(\delta^2\right) = \nu c x\left(\frac{39}{560} - \frac{3}{1120}\frac{\delta^2 c}{\nu} - \frac{1}{672}\left(\frac{\delta^2 c}{\nu}\right)^2\right) \tag{86}$$

$$f_2\left(\delta^2\right) = \nu^2\left[\frac{3}{2} - \frac{113}{280}\left(\frac{\delta^2 c}{\nu}\right) + \frac{41}{1680}\left(\frac{\delta^2 c}{\nu}\right)^2 + \frac{1}{840}\left(\frac{\delta^2 c}{\nu}\right)^3\right] \tag{87}$$

$$\frac{d}{dx}\frac{\delta^2 c}{\nu} = \frac{1}{x}\frac{\left[\frac{3}{2} - \frac{113}{280}\left(\frac{\delta^2 c}{\nu}\right) + \frac{41}{1680}\left(\frac{\delta^2 c}{\nu}\right)^2 + \frac{1}{840}\left(\frac{\delta^2 c}{\nu}\right)^3\right]}{\left[\frac{39}{560} - \frac{3}{1120}\frac{\delta^2 c}{\nu} - \frac{1}{672}\left(\frac{\delta^2 c}{\nu}\right)^2\right]} \tag{88}$$

$$\delta_{i+1}^2 = \frac{f_2\left(\delta_i^2\right)}{f_1\left(\delta_i^2\right)}\Delta x + \delta_i^2 \tag{89}$$

This equation can also be solved using the Euler scheme. There is, however, one important difference with the numerical solution for a flat plate at zero incidence. For that case the initial condition at *x*=0 was chosen as $\delta_0^2 = 0$, which was easy to implement. In the case of stagnation point flow, however, we do not know the initial value for $\frac{\delta^2 c}{\nu}$. However, as we saw from Blasius' solution, the boundary

layer thickness should remain constant, so we want to find $\frac{d}{dx}\frac{\delta^2 c}{\nu}=0 \rightarrow \frac{f_2\left(\frac{\delta^2 c}{\nu}\right)}{f_1\left(\frac{\delta^2 c}{\nu}\right)}=0$. This will only happen if $f_2\left(\frac{\delta^2 c}{\nu}\right)=0$. We can find that $\left[\frac{3}{2}-\frac{113}{280}\left(\frac{c\delta^2}{\nu}\right)+\frac{41}{1680}\left(\frac{c\delta^2}{\nu}\right)^2+\frac{1}{840}\left(\frac{c\delta^2}{\nu}\right)^3\right]=g=0$ should give the constant thickness of the boundary layer of the stagnation point flow. However, the similarity constant $\left(\frac{c\delta^2}{\nu}\right)$ in this equation, can only have positive values. In figure 3.2 the function g is shown against the similarity constant. It can be calculated that g is never equal to zero for positive similarity constants.

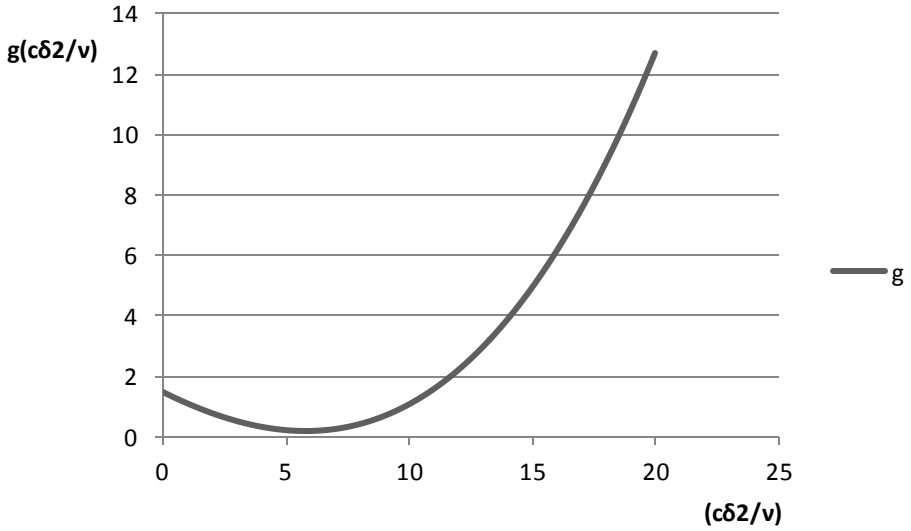

Figure 3.2 plot of the function g

In this plot it can be seen that the function does have a minimum value. This can be calculated to be 0.2, for $\left(\frac{c\delta^2}{\nu}\right)=5.8$. This would correspond with $\delta=2.4\sqrt{\frac{\nu}{c}}$.

3.3 Conclusion

Using the numerical solution for the flow over a flat plate at zero incidence it was shown that the numerical solution to the von Kármán integral momentum equation has a small error compared to the analytical solution of Blasius. However, this is just a small error in the boundary layer thickness and the numerical solution gives a good approximation of Blasius' solution. Because of this we can apply the von Kármán integral momentum equation to problems that cannot be solved analytically and expect the solution to be close to the exact solution as well. For Blasius' solution it was shown that the boundary layer for stagnation point flow on a flat plate perpendicular to the fluid stream has a constant boundary layer thickness. However, for the von Kármán integral momentum equation, no

such solution can be found. This means that the von Kármán integral momentum equation for stagnation point flow cannot be used to calculate the stagnation point boundary layer thickness for blunt objects with the stagnation point surface perpendicular to the free stream.

4. The experiment

The experiment concerns a flat plate with a thickness of 18 mm that is placed in the silent wind tunnel at zero degree angle of attack with respect to the free stream. To make sure that the boundary layer development is the same as for the flat plate of infinitesimal thickness that is considered in theory a specially developed leading edge(the nose) is attached to the plate. Using hot wire anemometry the velocity will be measured on the lower side of the plate, at several positions along the plate and several distances from the plate. Using these measurements the velocity profile can be constructed for different positions along the plate. Using the same free stream conditions in the von Kármán integral momentum equation found earlier, a velocity profile can be determined numerically. Then the theoretical and measured result can be compared.

Measurements will be carried out at three different *x*-positions along the plate. Three different free stream velocities have been used so a total of nine measurements have been carried out.

4.1 The windtunnel

The wind tunnel in which this experiment will be conducted is the silent wind tunnel of the University of Twente. This consists of a rectangular test section of 0.9x0.7 m^2, which is placed inside a closed anechoic room measuring 6x6 m^2 with a height of 4 m. Wind speed is created using a centrifugal fan. The speed can be adjusted by varying the input frequency. The tunnel can reach speeds of up to 65 m/s.

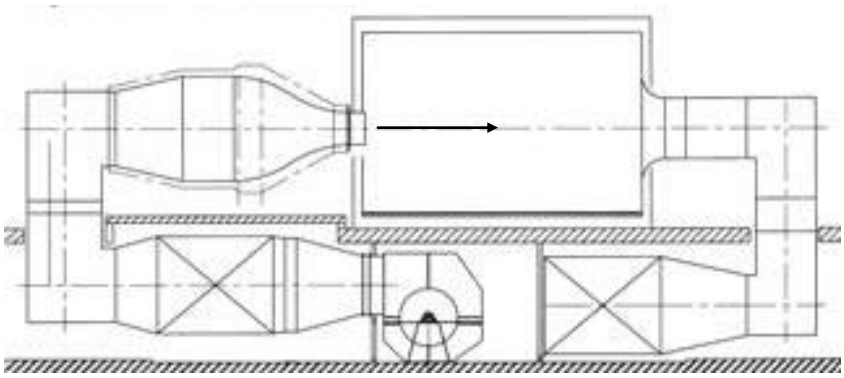

Figure 4.1 The silent wind tunnel of the University of Twente

4.2 The nose

The nose attached to the flat plate needs to have a specific design. If a round edge with a constant radius, i.e. a semi-circle, is used, the second derivative of the contour is discontinuous at the location where the nose is attached to the flat plate. This will lead to a disturbance in the velocity and pressure distributions. The present design is such that at the location where the specific blunt nose is attached to the flat plate, the geometry is continuous in function value, slope, curvature and derivative of the curvature with respect to the x-coordinate. This can be accomplished when the shape of the nose is designed using cubic Hermite polynomials. Then the nose will look like shown in figure 4.2. The nose has been machined by a specialized company.

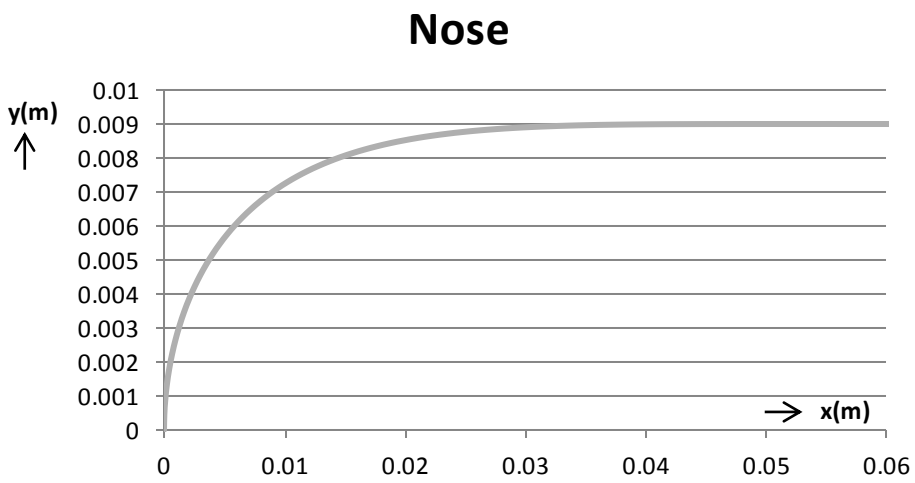

Figure 4.2 geometry of the leading edge of the flat plate

4.3 Hot wire anemometer

The velocity will be measured using hot wire anemometry. A probe with a heating element is placed in the fluid stream. This probe is connected to a constant temperature anemometer, or CTA. The CTA sends a current to the heating element to keep the temperature constant. Because of the fluid flowing past the heating element in the probe it will cool. The amount of current needed is a measure for the cooling of the element. Because the element is cooled only by the fluid flow, this is also a measure for the velocity of the fluid. The probe that will be used is the Dantec 55P11. This has platinum plated tungsten wire with a length of 1.25 mm and a diameter of 5µm. The length of the prongs holding the wire is 5 mm.

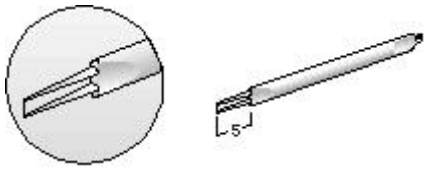

Figure 4.3 the Dantec 55P11

This probe is placed in a probe support which is connected to a wing like strut to reduce the disturbance of the flow as much as possible. The strut is fitted with a plate which can slide over the bottom of the wind tunnel test section so the strut can be translated in *x* and *z* direction without altering flow properties because of a hole in the bottom of the test section. The strut can translate in *y* direction (i.e. vertical direction) using a precise traversing mechanism, such that translations with a resolution of 0.1mm are possible.

5. Results of the experiment

In this chapter the results of the experiment will be discussed. There is a change from the description that was made earlier, however. Because of a holiday period during the planning, the special leading edge was not ready in time to be used in the experiments. The experiment is thus carried out with the rounded nose with a constant radius of curvature.

The experiment was conducted at a temperature of 23°C. $\mu = 1.81 \cdot 10^{-5}$ Pas; $\rho = 1.29$ kg/m^3. Measurements were done for a free stream velocity of 2 m/s, 5 m/s and 10 m/s. For each velocity, the velocity profile was measured at three different locations, namely *x*=18.1 cm; *x*=19.1 cm and *x*=20.1 cm where *x*=0 is the start of the flat part of the plate. With a thickness of 18 mm, the radius of the round edge is 9 mm so the start of the flat part is 9 mm downstream of the leading edge of the plate. The data that is collected in the experiments will be presented using graphs.

At first the velocity profile was measured for one location, namely x=19.1 cm for al velocities. After that, the velocity profile was measured for the other two positions. During the measurements for *x*=18.1 cm second location with a velocity of 5 m/s the probe broke. A new probe was calibrated and for accuracy al positions were measured again for the 5 m/s and 10 m/s free stream velocity.

5.1 Velocity of 2 m/s

Below the graphs are shown for a free stream velocity of 2 m/s. The dots shown in the graph are the measured data, the line which is shown is an approximation of the resulting velocity profile.

5.1.1 X=18.1cm

The Reynolds number for this flow is Re_x=25800, which is much lower than the critical Reynolds number, so a laminar velocity profile is expected. The approximation which is shown in the graph is calculated by taking a running 5-point average.

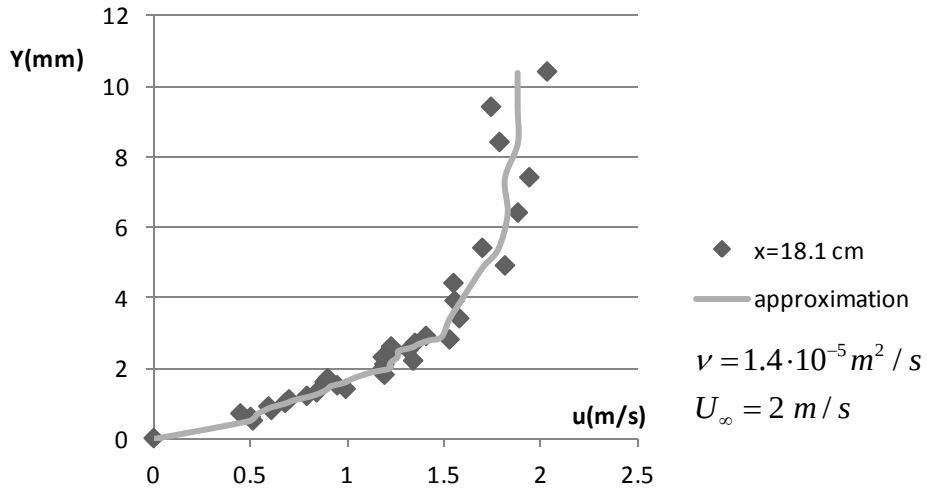

Figure 5.1 Velocity profile for x=18.1 cm and U=2 m/s; Re_x=25800
Note that the point at y=0 is indicated for clarity

This looks like the Blasius' solution velocity profile for the flow in a laminar boundary layer.

5.1.2 X=19.1cm

The Reynolds number for this flow is Re_x=27225, which is again much lower than the critical Reynolds number, so again a laminar velocity profile is expected.

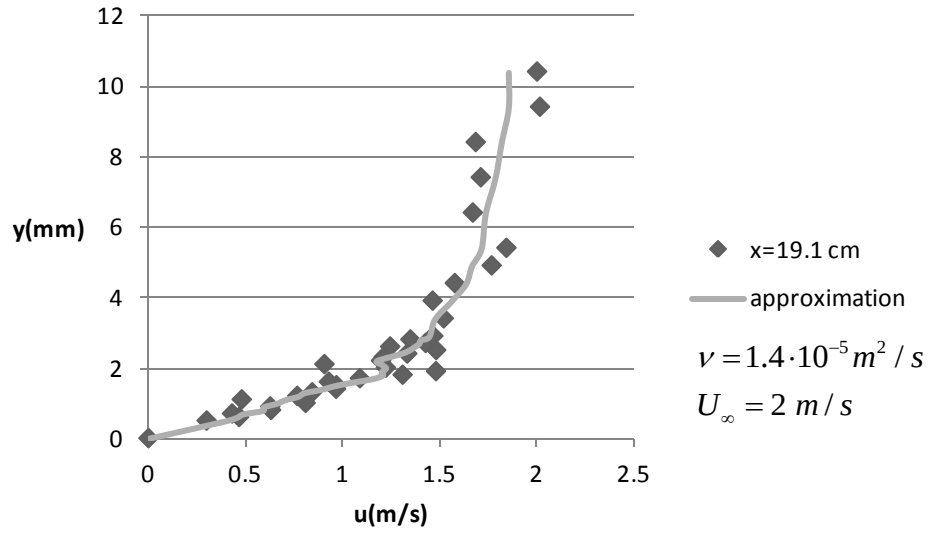

Figure 5.2 Velocity profile for x=19.1 cm and U=2 m/s; Re_x=27225 again the point at y=0 is indicated.

5.1.3 X=20.1cm

The Reynolds number for this flow is Re_x=28650, so a laminar velocity profile is expected for this situation as well.

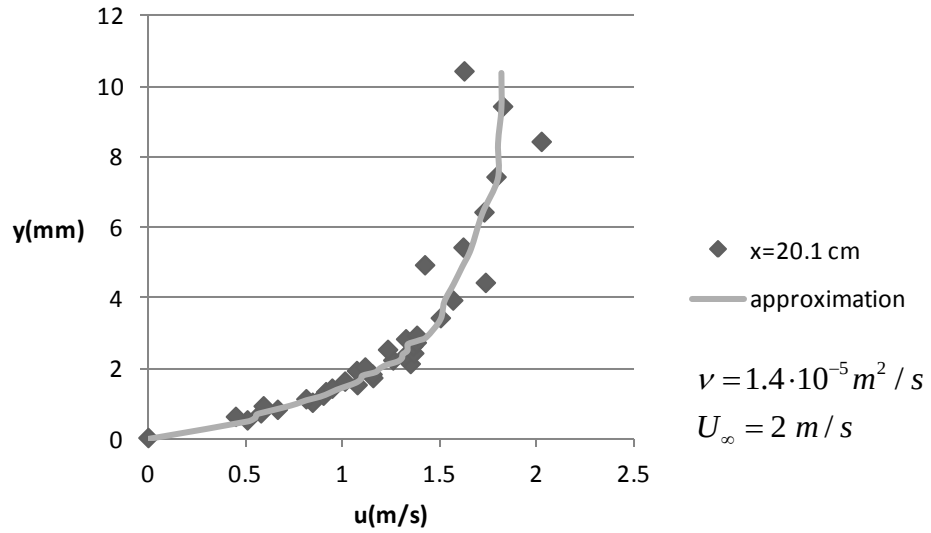

Figure 5.3 Velocity profile for x=20.1 cm and U=2 m/s; Re_x=28650

This also looks very similar to Blasius' solution for a laminar boundary layer. If the result of these 3 situations are plotted against the parameter η, they can be compared. This is done in figure 5.4. If we compare the results for these 3 situations, it can be seen that the difference between the results is not large. So for the results of the 5 m/s velocity and 10 m/s velocity we will suffice with a single graph.

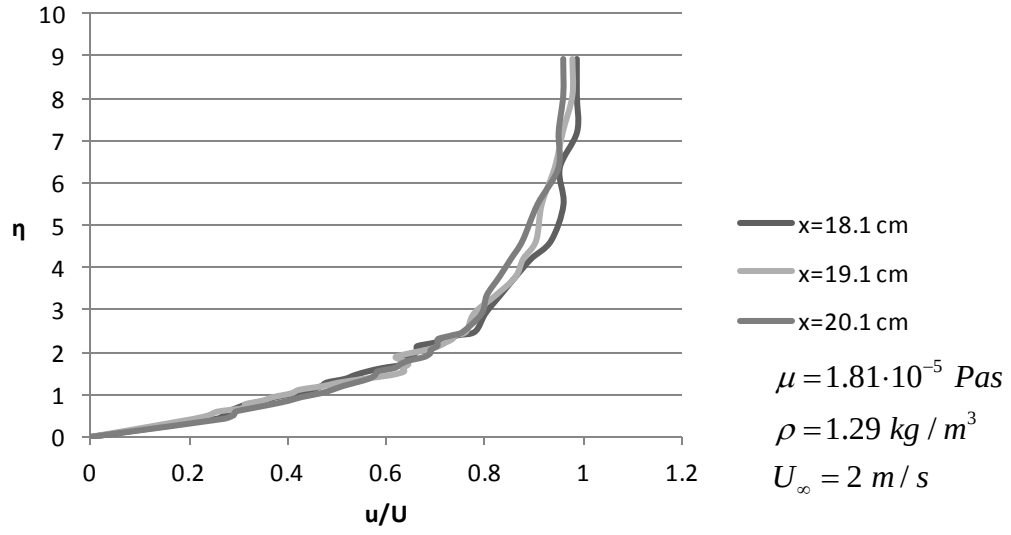

Figure 5.4 the approximations for the three velocity profiles for U=1.9 m/s shown in dimensionless parameters

5.2 5 m/s

Again a graph will be shown with the results of the velocity measurements. This time for a free stream velocity of 5 m/s. Only one result will be shown because of assumed similarity. In this case the measurement for x=19.1 cm will be used. The Reynolds number for this flow is Re_x=61123, so still a laminar flow regime is expected. The approximation of the velocity profile is calculated in the same way as for the 2 m/s case.

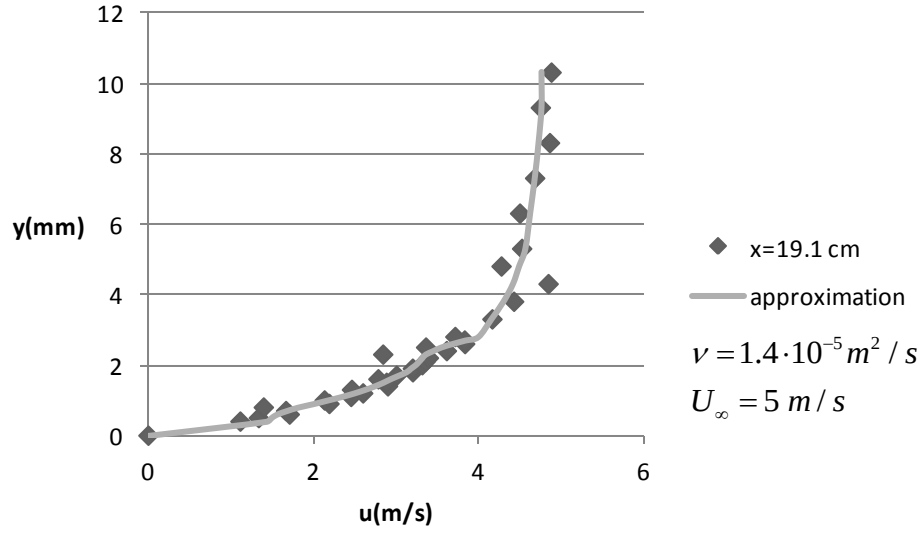

Figure 5.5 the approximation of the velocity profile for x=19.1 cm for U=5 m/s; Re_x=61123

5.3 10 m/s

For the results of the measurements at a velocity of 10 m/s also one graph will be shown. Again the measurement for x=19.1 cm. The Reynolds number for this situation is Re_L=122246. Because of this

still a laminar boundary layer is expected. In this case, the measured data shows not much scatter, so no approximation is added to the graph.

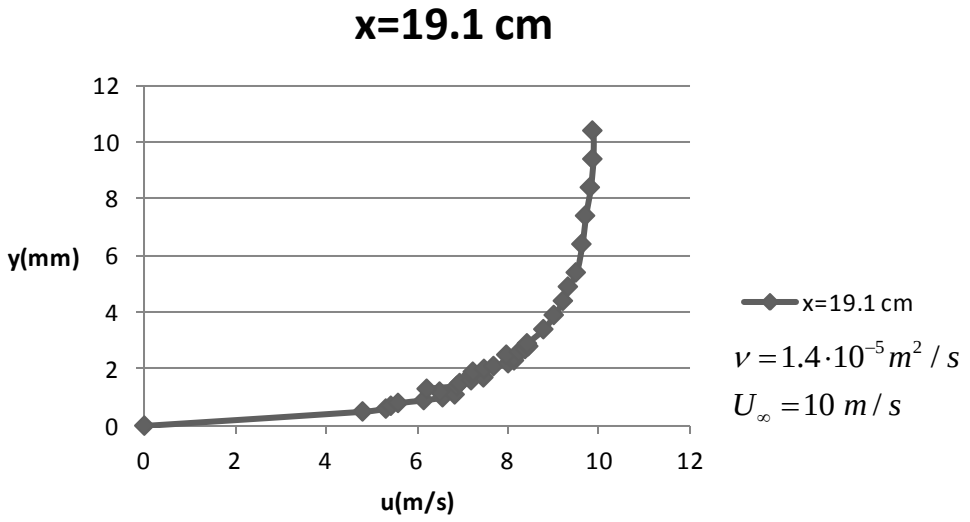

Figure 5.6 the approximation of the velocity profile for x=19.1 cm for U=10 m/s; Re_x=122246

6. Comparison of theoretical and experimental results

In this chapter a comparison will be made between the theoretical results and the experimental results. Before that can be done, however, the numerical boundary layer needs to be obtained for the flat plate with the specially designed leading edge. To do this the pressure distribution along the leading edge is used to calculate the tangential velocity along the surface. This can be done using Bernoulli's equation in the form of the pressure coefficient

$$c_p \equiv \frac{p - p_\infty}{\frac{1}{2}\rho_\infty U_\infty^2} = 1 - \frac{U^2}{U_\infty^2} \rightarrow U(\text{tangential}) = U_\infty \sqrt{1 - C_p} \tag{90}$$

In figure 6.1 the tangential velocity is plotted against the distance from the leading edge. This is for a free stream velocity of 2 m/s, the length of the leading edge is 0.054 m. The pressure distribution used for these calculations is generated by Hein de Vries and was shared via private communication. It can be found in appendix A.

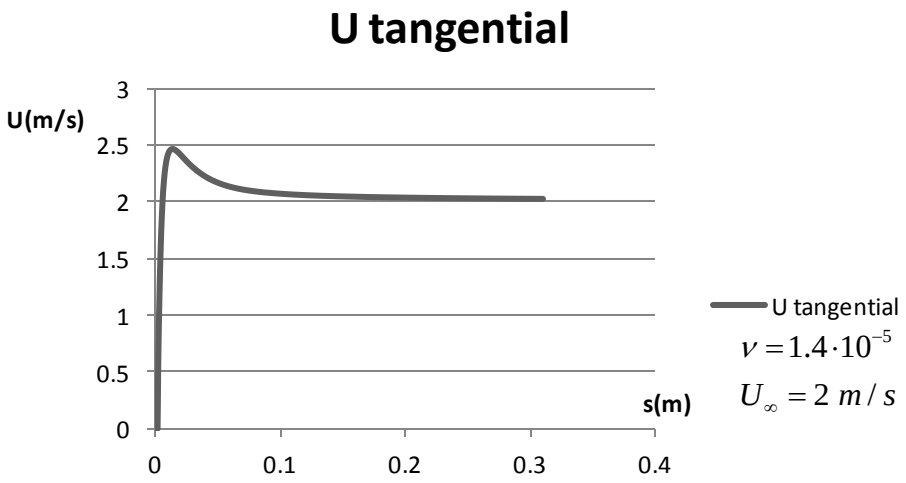

Figure 6.1 Tangential velocity as function of arc lengths along the leading edge and first part of the flat plate. The flat plate starts at s=0.057m

As can be seen in the figure, there is a velocity gradient along the leading edge and along a part of the flat plate. This velocity gradient can be calculated. This can then be used in the von Kármán integral momentum equation(72). Solving this equation for the boundary layer thickness of a position *s* will give the velocity profile in the boundary layer at that position. The same can be done for Blasius' solution. Both the numerical solution for the boundary layer thickness and Blasius' solution are displayed in figure 6.2. This result is for a free stream velocity of 2 m/s. For higher free stream velocities, the same profile was found except for the thickness being smaller, following the rules we found from the similarity solution.

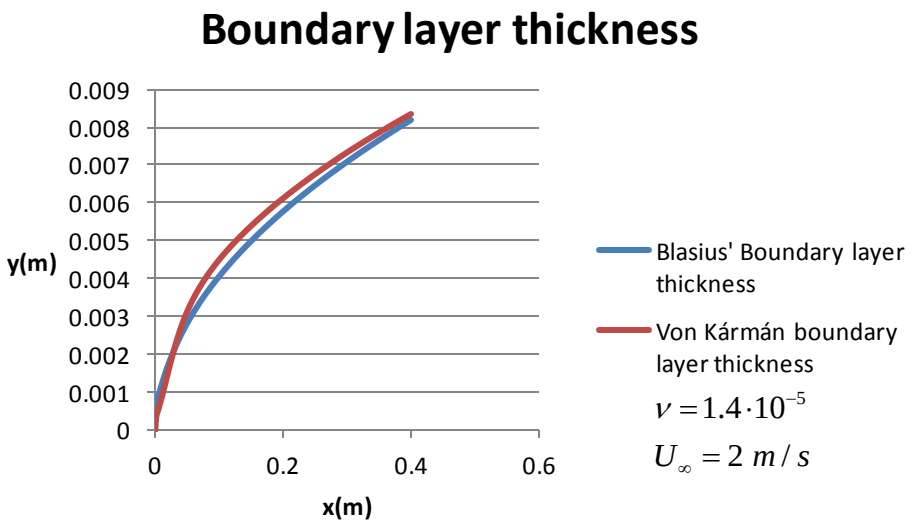

Figure 6.2 boundary layer thickness along the flat plat with the special leading edge compared to Blasius' solution

6.1 Boundary layer velocity profile

Because of Blasius's solution being the analytical solution, the measured data will be plotted against the velocity profile according to Blasius. Blasius' solution will be plotted as $f'(\eta)$ against η so the results can be compared independent of x.

6.1.1 Velocity profile 2m/s

First the result for a velocity of 2 m/s will be shown.

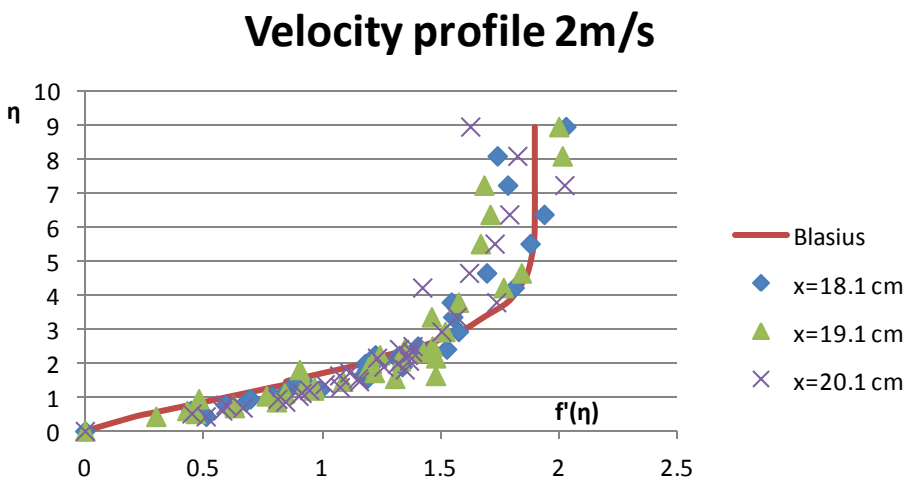

Figuur 6.3 The velocity profile according to Blasius' solution and the measurements at different x-stations for U=2 m/s

As can be seen the result of the different measurements are comparable. The velocity profile also looks similar to the result of Blasius' equation. The test results show some scatter. This can be explained by the fact that the free stream velocity generated by the wind tunnel is not precisely constant at these low speeds.

6.1.2 Velocity profile 5 m/s

The next is the velocity profile for a free stream velocity of 5 m/s.

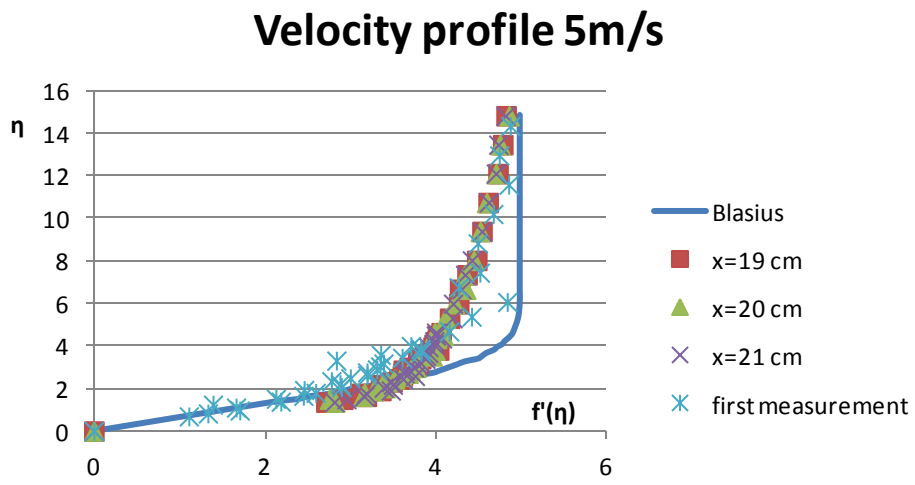

Figure 6.4 The velocity profile according to Blasius' solution and the measurements at different x-stations for U=5 m/s

It can be seen that the different measurement results show a nearly similar velocity profile, even the results of the two different probes. However, this time the shape of the measured velocity distribution looks more like a turbulent boundary layer velocity profile. This might be the effect of the blunt leading edge of the plate used in the experiment.

6.1.3 Velocity profile 10 m/s

The last test results are for a free stream velocity of 10 m/s.

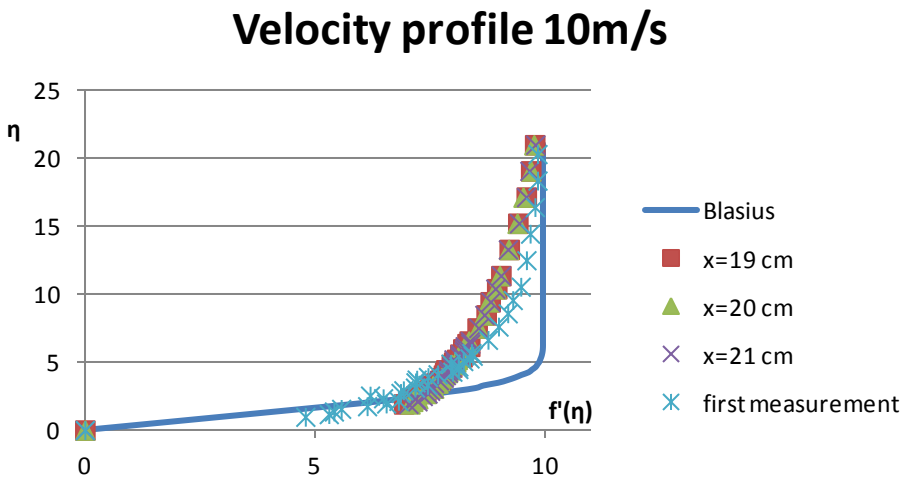

Figure 6.5 The velocity profile according to Blasius' solution and the measurements at different x-stations for U=10 m/s

Just as with the measurements for a free stream velocity of 5m/s, the measurements for a free stream velocity of 10 m/s show a nearly similar velocity profile, but again it differs from Blasius' velocity profile for a laminar flow.

7. Conclusion

In this study a comparison has been made between analytical and numerical results for the velocity profile of a fluid stream over a flat plate. Besides that a comparison is made between the analytical result and the measurements with a test set-up in a wind tunnel. The conclusions that can be drawn from these experiments will be stated here.

7.1 Analytical versus numerical results

It was shown in chapter 3.1 that for the simplest case, the flat plate of infinitesimal thickness, the numerical solution is similar to the analytical solution. The difference between the thickness of the boundary layer from the numerical solution is 5.5% smaller than that from the analytical solution. In chapter 3.2 the analytical and numerical solutions of the stagnation point flow on a flat plate are compared. It was found that the numerical solution cannot be similar to the analytical solution. In chapter 6, the solution of the von Kármán integral momentum equation and Blasius' solution were compared for the actual test set-up. This again gave comparable results for the boundary layer thickness. From this it can be concluded that the von Kármán integral momentum equation does give reasonable results for flat plate type of flows, but is not useful for stagnation type of flows.

7.2 Analytical versus measured results

In chapter 6 the analytical result of Blasius' solution is compared to the data measured in a wind tunnel under similar conditions. Although the specially designed leading edge was not used in the present experiment, the results at low velocity are nearly similar to the analytical result. However, if the velocity is increased, the measurement results show a velocity profile that appears to indicate that the boundary layer is turbulent. According to the analytical method a laminar boundary layer is still expected. Thus we see a difference in theory and practice at higher velocities. This is expected to be partially caused by the leading edge which is different in the theory and practice. Also other factors could have influence, such as the turbulence of the flow in the windtunnel, misalignment of the plate, etc. It can be concluded from this that a boundary layer that should be laminar according to theory can be turbulent in practice, thus giving a thicker boundary layer and a different velocity profile.

Bibliography

1. Cengel, Y.A. **Heat Transfer: A Practical Approach.** 2nd ed. McGraw-Hill

2. ANDEL, K. van. **SWO Stromingsleer & warmteoverdracht college 7 and 8.**

3. ANDERSON, J. D. **Fundamentals of Aerodynamics.** Singapore: McGraw-Hill, 2007

4. http://www.solutioninn.com/engineering/chemical-engineering/transport-phenomena/potential-flow-near-a-stagnation-point-fig-4b6--a-show

5. KUNDU, P. K. & COHEN, I. M. **Fluid Mechanics.** 4th ed. Academic Press.

Appendix A: Pressure distribution along the plate

x	y	Cp
6.48E-07	0	1.043979
2.81E-05	0.000449	1.015285
0.00011	0.000903	0.935395
0.000249	0.001357	0.817208
0.000439	0.001806	0.67428
0.000681	0.002244	0.519638
0.00097	0.00267	0.364989
0.001303	0.003081	0.21874
0.001677	0.003475	0.085256
0.002089	0.003853	-0.03332
0.002538	0.004213	-0.13614
0.00302	0.004556	-0.22329
0.003534	0.004881	-0.29559
0.004078	0.005189	-0.35438
0.004653	0.005481	-0.40114
0.005256	0.005756	-0.43742
0.005887	0.006017	-0.46469
0.006546	0.006262	-0.48433
0.007232	0.006494	-0.49752
0.007945	0.006712	-0.50526
0.008687	0.006917	-0.50839
0.009455	0.00711	-0.50764
0.010253	0.00729	-0.50365
0.011078	0.007459	-0.49698
0.011934	0.007616	-0.48809
0.012819	0.007763	-0.47739
0.013735	0.007899	-0.46522
0.014683	0.008025	-0.45192
0.015664	0.008141	-0.43775
0.016679	0.008248	-0.42292
0.017729	0.008346	-0.40763
0.018816	0.008436	-0.39205
0.019941	0.008517	-0.37632
0.021106	0.00859	-0.36056
0.022313	0.008656	-0.34488
0.023562	0.008714	-0.32939
0.024857	0.008765	-0.31414
0.026199	0.00881	-0.29917
0.027591	0.008849	-0.28453
0.029035	0.008883	-0.27025
0.030534	0.008911	-0.25634
0.03209	0.008934	-0.24284
0.033707	0.008953	-0.22977
0.035387	0.008968	-0.21716
0.037135	0.008979	-0.20503
0.038953	0.008987	-0.19339
0.040846	0.008992	-0.18227
0.042819	0.008996	-0.17166
0.044875	0.008998	-0.16157
0.04702	0.008999	-0.15198
0.049259	0.009	-0.14291
0.051599	0.009	-0.13433
0.054045	0.009	-0.12625
0.056604	0.009	-0.11866
0.059284	0.009	-0.11154
0.062093	0.009	-0.10489
0.065041	0.009	-0.09868
0.068136	0.009	-0.09289
0.071389	0.009	-0.08751
0.074813	0.009	-0.0825
0.078421	0.009	-0.07786
0.082225	0.009	-0.07357
0.086244	0.009	-0.06957
0.090493	0.009	-0.06576
0.094993	0.009	-0.06222
0.099493	0.009	-0.05907
0.103994	0.009	-0.05624
0.108495	0.009	-0.05368
0.112999	0.009	-0.05137
0.117505	0.009	-0.04926
0.122013	0.009	-0.04733
0.126525	0.009	-0.04555
0.131041	0.009	-0.04391
0.135561	0.009	-0.04239
0.140086	0.009	-0.04097
0.144617	0.009	-0.03965
0.149154	0.009	-0.03841
0.153698	0.009	-0.03725
0.158249	0.009	-0.03616
0.162809	0.009	-0.03513
0.167376	0.009	-0.03415
0.171953	0.009	-0.03323
0.176539	0.009	-0.03235
0.181136	0.009	-0.03152
0.185743	0.009	-0.03073
0.190361	0.009	-0.02997
0.194992	0.009	-0.02925
0.199634	0.009	-0.02857
0.20429	0.009	-0.02791
0.20896	0.009	-0.02727
0.213644	0.009	-0.02666
0.218342	0.009	-0.02607
0.223056	0.009	-0.02549
0.227786	0.009	-0.02494
0.232533	0.009	-0.02439
0.237297	0.009	-0.02386
0.242078	0.009	-0.02335
0.246878	0.009	-0.02289
0.251697	0.009	-0.02244
0.256535	0.009	-0.02201
0.261394	0.009	-0.02159
0.266273	0.009	-0.02119
0.271174	0.009	-0.0208
0.276096	0.009	-0.02042
0.281042	0.009	-0.02005
0.28601	0.009	-0.01969
0.291002	0.009	-0.01934
0.296019	0.009	-0.019
0.301061	0.009	-0.01867
0.306129	0.009	-0.01835
0.311223	0.009	-0.01804
0.316343	0.009	-0.01773
0.321492	0.009	-0.01743
0.326669	0.009	-0.01715
0.331875	0.009	-0.01686
0.33711	0.009	-0.01659
0.342375	0.009	-0.01632
0.347672	0.009	-0.01606
0.353	0.009	-0.01581
0.35836	0.009	-0.01556
0.363753	0.009	-0.01532
0.369179	0.009	-0.01508
0.37464	0.009	-0.01485
0.380136	0.009	-0.01462
0.385667	0.009	-0.01441
0.391235	0.009	-0.01419

x	y	Cp
0.396839	0.009	-0.01398
0.402481	0.009	-0.01378
0.408162	0.009	-0.01358
0.413881	0.009	-0.01339
0.419641	0.009	-0.0132
0.425441	0.009	-0.01301
0.431282	0.009	-0.01283
0.437165	0.009	-0.01265
0.443091	0.009	-0.01248
0.44906	0.009	-0.0123
0.455074	0.009	-0.01213
0.461132	0.009	-0.01197
0.467237	0.009	-0.0118
0.473387	0.009	-0.01164
0.479585	0.009	-0.01148
0.485831	0.009	-0.01133
0.492125	0.009	-0.01117
0.49847	0.009	-0.01102
0.504864	0.009	-0.01088
0.51131	0.009	-0.01073
0.517807	0.009	-0.01059
0.524358	0.009	-0.01045
0.530962	0.009	-0.01031
0.53762	0.009	-0.01017
0.544334	0.009	-0.01004
0.551104	0.009	-0.00991
0.55793	0.009	-0.00978
0.564815	0.009	-0.00965
0.571758	0.009	-0.00952
0.57876	0.009	-0.00939
0.585823	0.009	-0.00927
0.592948	0.009	-0.00915
0.600134	0.009	-0.00903
0.607383	0.009	-0.00891
0.614697	0.009	-0.00879
0.622075	0.009	-0.00868
0.629519	0.009	-0.00857
0.63703	0.009	-0.00846
0.644608	0.009	-0.00835
0.652255	0.009	-0.00824
0.659972	0.009	-0.00813
0.667759	0.009	-0.00803
0.675617	0.009	-0.00793
0.683548	0.009	-0.00782

x	y	Cp
0.691553	0.009	-0.00772
0.699631	0.009	-0.00763
0.707786	0.009	-0.00753
0.716017	0.009	-0.00743
0.724325	0.009	-0.00734
0.732712	0.009	-0.00725
0.741178	0.009	-0.00716
0.749725	0.009	-0.00707
0.758354	0.009	-0.00698
0.767066	0.009	-0.0069
0.775861	0.009	-0.00681
0.784742	0.009	-0.00672
0.793708	0.009	-0.00664
0.802762	0.009	-0.00655
0.811904	0.009	-0.00647
0.821136	0.009	-0.00639
0.830458	0.009	-0.00631
0.839872	0.009	-0.00623
0.849379	0.009	-0.00615
0.85898	0.009	-0.00607
0.868677	0.009	-0.00599
0.87847	0.009	-0.00592
0.888361	0.009	-0.00584
0.89835	0.009	-0.00578
0.908441	0.009	-0.00571
0.918632	0.009	-0.00564
0.928927	0.009	-0.00558
0.939325	0.009	-0.00552
0.949829	0.009	-0.00546
0.960439	0.009	-0.0054
0.971158	0.009	-0.00534
0.981986	0.009	-0.00529
0.992925	0.009	-0.00523
1.003975	0.009	-0.00516
1.015139	0.009	-0.00509
1.026418	0.009	-0.00502
1.037814	0.009	-0.00494
1.049327	0.009	-0.00485
1.060959	0.009	-0.00475
1.072711	0.009	-0.00465
1.084586	0.009	-0.00454
1.096584	0.009	-0.00441
1.108707	0.009	-0.00432
1.120957	0.009	-0.00427

x	y	Cp
1.133334	0.009	-0.00423
1.145842	0.009	-0.00419
1.15848	0.009	-0.00414
1.171251	0.009	-0.0041
1.184157	0.009	-0.00405
1.197198	0.009	-0.00401
1.210377	0.009	-0.00396
1.223695	0.009	-0.00391
1.237154	0.009	-0.00386
1.250756	0.009	-0.00382
1.264502	0.009	-0.00377
1.278394	0.009	-0.00372
1.292433	0.009	-0.00368
1.306622	0.009	-0.00363
1.320962	0.009	-0.00358
1.335455	0.009	-0.00354
1.350103	0.009	-0.00349
1.364908	0.009	-0.00345
1.379871	0.009	-0.0034
1.394995	0.009	-0.00335
1.41028	0.009	-0.00331
1.42573	0.009	-0.00326
1.441346	0.009	-0.00322
1.45713	0.009	-0.00317
1.473084	0.009	-0.00313
1.48921	0.009	-0.00308
1.50551	0.009	-0.00304
1.521987	0.009	-0.00299
1.538641	0.009	-0.00295
1.555475	0.009	-0.0029
1.572492	0.009	-0.00286
1.589693	0.009	-0.00281
1.60708	0.009	-0.00277
1.624657	0.009	-0.00273
1.642424	0.009	-0.00269
1.660384	0.009	-0.00264
1.67854	0.009	-0.0026
1.696893	0.009	-0.00256
1.715446	0.009	-0.00252
1.734202	0.009	-0.00248
1.753162	0.009	-0.00243
1.772329	0.009	-0.00239
1.791706	0.009	-0.00235
1.811294	0.009	-0.00231

x	*y*	*Cp*
1.831096	0.009	-0.00228
1.851115	0.009	-0.00224
1.871353	0.009	-0.0022
1.891813	0.009	-0.00216
1.912497	0.009	-0.00212
1.933408	0.009	-0.00208
1.954549	0.009	-0.00204
1.975921	0.009	-0.00201
1.997529	0.009	-0.00197
2.019373	0.009	-0.00193
2.041458	0.009	-0.0019
2.063786	0.009	-0.00186
2.08636	0.009	-0.00182
2.109182	0.009	-0.00179
2.132255	0.009	-0.00175
2.155583	0.009	-0.00171
2.179168	0.009	-0.00167
2.203013	0.009	-0.00163
2.227121	0.009	-0.00159
2.251496	0.009	-0.00155
2.276139	0.009	-0.00152
2.301055	0.009	-0.00148
2.326245	0.009	-0.00144
2.351715	0.009	-0.00141
2.377466	0.009	-0.00138
2.403502	0.009	-0.00135
2.429826	0.009	-0.00132
2.456441	0.009	-0.00129
2.483352	0.009	-0.00126
2.51056	0.009	-0.00123
2.53807	0.009	-0.0012
2.565884	0.009	-0.00117
2.594007	0.009	-0.00114
2.622442	0.009	-0.0011
2.651193	0.009	-0.00107
2.680262	0.009	-0.00104
2.709654	0.009	-0.001
2.739373	0.009	-0.00097
2.769421	0.009	-0.00093
2.799803	0.009	-0.0009
2.830523	0.009	-0.00086
2.861584	0.009	-0.00083
2.892991	0.009	-0.00079
2.924746	0.009	-0.00076

x	*y*	*Cp*
2.956855	0.009	-0.00073
2.989321	0.009	-0.0007
3.022149	0.009	-0.00067
3.055341	0.009	-0.00064
3.088903	0.009	-0.00061
3.122839	0.009	-0.00057
3.157153	0.009	-0.00054
3.191849	0.009	-0.0005
3.226931	0.009	-0.00046
3.262404	0.009	-0.00042
3.298273	0.009	-0.00038
3.334541	0.009	-0.00035
3.371214	0.009	-0.00034
3.408295	0.009	-0.00034
3.44579	0.009	-0.00036
3.483703	0.009	-0.00044
3.52204	0.009	-0.00058
3.560804	0.009	-0.00137
3.6	0.009	-0.00208